Environ. Sci. Technol. **1998**, *32,* 1948−1955

Fourier Transform Raman Spectroscopy of Sorbed HDTMA and the Mechanism of Chromate Sorption to Surfactant-Modified Clinoptilolite

ENID J. SULLIVAN,*,† DOUGLAS B. HUNTER,‡ AND ROBERT S. BOWMAN†

Department of Earth and Environmental Science and Geophysical Research Center, New Mexico Institute of Mining and Technology, Socorro, New Mexico 87801, and Division of Biogeochemistry, University of Georgia, Savannah River Ecology Laboratory, Aiken, South Carolina 29801

We examined sorption of the cationic surfactant hexadecyltrimethylammonium bromide (HDTMA) to clinoptilolite zeolite and the subsequent sorption of the chromate anion to surfactant-modified zeolite (SMZ). We used Fourier transform (FT) Raman spectroscopy and batch sorption methods to elucidate the structure of sorbed HDTMA and to determine the mechanisms of chromate sorption. At high HDTMA loading levels (above the zeolite's external cation exchange capacity, ECEC), the Raman spectra indicated that sorbed HDTMA was similar in conformation to solution micelles and, thus, may contain anion exchange sites. Sorbed HDTMA showed less structuring of tail groups and a decrease in head group hydration. At lower loadings, the sorbed HDTMA tail groups tended to have more disorder, similar to solution monomers. When HDTMA loading rates were greater than 100% of the ECEC, chromate sorbed onto SMZ with near-equivalent Br^- counterion exchange. A peak in the Raman spectrum at 902 cm^{-1} indicated the presence of sorbed $Cr_2O_7^{2-}$, although no bulk solution oligomerized chromate species should have been present at a solution pH of 7. A 30 cm^{-1} shift in the ν_1 peak for sorbed versus solution chromate may indicate that surface-enhanced Lewis acid−base interactions were responsible for some chromate sorption in addition to the predominant anion-exchange mechanism.

Introduction

Surfactant-modified zeolite (SMZ) has potential use as a sorbent for toxic compounds from contaminated waters, in subsurface permeable barriers, or in ex-situ water treatment systems. SMZ can sorb organic compounds as well as inorganic cations and oxyanions from water (*1*−*3*). Partitioning is responsible for organic sorption by SMZ while transition metal cation sorption is generally unaffected (*1*). The conformation and quantity of surfactant on the surface as well as complex interactions between the surface and the surfactant are potentially responsible for the ability of the surface to retain oxyanions (*2*). One proposed mechanism is retention of the oxyanions via anion exchange with counterions on the external portion of a surfactant bilayer or admicelles (*4*). Another proposed mechanism is a surface-precipitation reaction (*2*). The presence of admicelles versus a monolayer is thus important because admicelle presence implies the presence of anion exchange sites.

The Raman spectrum arises from changes in molecular polarizability, while the infrared (IR) spectrum arises from changes in dipole moment during visible, infrared, or ultraviolet-induced molecular vibrations (*5*). Peaks can be recorded for both IR and Raman at some frequencies while other vibrations may be mutually exclusive. Changes in the chemical environment that affect the polarizability of a bond will shift or remove a band in a Raman spectrum. Low concentrations of the bond type also can cause apparent removal of a band because of low signal-to-noise ratios. Previously, Fourier transform IR (FTIR) methods have been used to characterize surfactant structure in micelles and on surfaces (*6*−*8*), and interpretations of these data have relevance to FT-Raman spectral interpretation. A number of atomic groups in organic compounds produce vibrations at characteristic wavenumbers for both Raman and IR methods (*9, 10*). These include, for example, the CH_2 stretching modes between 3000 and 2800 cm^{-1} and the CH_2 bending modes between 1470 and 1400 cm^{-1}.

In biological and chemical systems, FT-Raman spectroscopy has been used successfully to characterize the structural conformation, functionalities, and molecular composition of lipid bilayers and surfactant mono- and bilayers, including the interdigitization of lipid and surfactant chains or tail groups in bilayers (*11*−*14*). Integrated band intensities, peak height ratios, and peak shifts were used to measure these properties. Particularly, the region between 3100−2800 cm^{-1} was used to examine the acyl or alkyl chain C−H stretching mode region to show bilayer perturbations (*11, 12*). This spectral region is also accepted in IR spectroscopy as a means of determining trans to gauche transitions based on band frequency shifts, such as during thermotropic phase transitions of sorbed fatty acids (*7*), and surfactant conformation changes at different coverages and wetting states on silica (*8*). These vibrations are important in that they can help measure the order/disorder, compactness, and crystallinity of the alkyl chain (*8, 13*). Comparable band shifts in the FT-Raman spectrum have been noted (*13, 14*).

Oxyanions such as chromate can produce strong peaks that exhibit band shifts and variations in intensity and height ratios depending upon the chemical environment before and after sorption. FT-Raman spectroscopy was chosen to probe surface interactions between zeolite, surfactant, and chromate because it can give information about binding between SMZ and chromate and the geometry of surfactant molecules and oxyanions. Anion-exchange sites for chromate sorption have been demonstrated to occur on surfactant bilayers on hexadecyltrimethylammonium (HDTMA)-modified zeolite (*15*). Alternately, hexavalent chromate may act as a Lewis base by donating an electron pair to acid sites present on the zeolite surface. The presence of Lewis acid sites on zeolites has been demonstrated (*16, 17*). These sites on adsorbates are known to affect the polarizability and dipole moment of the conjugate acid or base and, thus, the Raman and IR band frequencies (*10, 16, 18* and others cited therein). Lewis acid sites occur when the zeolites have been completely alkali-exchanged and dried under vacuum (*16, 18*). The presence

* Corresponding author present address: Bureau of Economic Geology, University of Texas at Austin, University Station Box X, Austin, TX 78713-8924; phone: (512)471-6285; fax: (512)471-0140; e-mail: sullivanj@begv.beg.utexas.edu.

† New Mexico Institute of Mining and Technology.

‡ University of Georgia.

S0013-936X(97)00898-5 CCC: $15.00 © 1998 American Chemical Society
Published on Web 05/15/1998

of the surfactant may substantially reduce the amount of near-surface water in aqueous systems, enhancing the relative acidity of such sites and subsequently promoting chromate sorption. The ultimate goal of this study was to determine what chromate sorption processes are occurring on the zeolite surface.

Near-infrared FT-Raman spectroscopy holds a number of advantages over conventional Raman techniques, including avoidance of sample fluorescence (*13*). The broad adsorption bands of water in IR spectra at 1640 and 3000−4000 cm^{-1} can obscure data from other sorbed compounds. This problem is eliminated in the near-IR FT-Raman spectrum, expanding the range of absorbance information. FT-Raman techniques can be used on wet surface-adsorbed samples, particularly because the Raman spectrum is principally a result of the sorbed material only (*5, 10*). This allows examination of the sorbed surfactant under in-situ conditions.

This paper describes spectroscopic and macroscopic methods used to examine interactions between a surfactant, HDTMA, and a natural clinoptilolite surface and the type of interaction occurring between the SMZ and chromate. FT-Raman spectroscopy was used to examine the structural characteristics of HDTMA sorbed to zeolite, HDTMA solutions, and the SMZ−chromate system. Sorption isotherms were used to quantify the amounts of HDTMA, HDTMA counterion (Br^-), and chromate retained by the SMZ to account for potential chromate sorption mechanisms.

Materials and Methods

Zeolite and Reagents. The zeolite used is a clinoptilolite-rich tuff from the St. Cloud mine in Winston, NM. It consists of about 74% clinoptilolite, 5% smectite, 10% quartz and cristobalite, 10% feldspar, and 1% illite, based on internal standard X-ray diffraction analysis (*19, 20*). We measured an external cation-exchange capacity (ECEC) of 70−90 mequiv/kg for the St. Cloud zeolite using a modification of the method of Ming and Dixon (*21*). The external surface area is exchanged with a large molecule such as *tert*-butyl ammonium ion, which cannot penetrate within the zeolite pore spaces. The internal surface area is then determined by difference using a small exchanging ion such as Cs^+. We also measured an external surface area of 15.7 m^2/g on a sample dried for 24 h at 200 °C using the BET nitrogen adsorption method, which has been shown to represent an external surface area (*4, 15*). The zeolite was sieved to a size range of 2 mm−150 μm prior to use. The HDTMA−Br^- was used as received (Sigma Chemicals, >99% purity). Reagent-grade K_2CrO_4 was also used as received (Baker Chemicals). All aqueous solutions were made with 18.2 MΩ cm^{-1} (ASTM Type I) water.

Sorption Experiments. For the sorption experiments, variable quantities (0.1−4 g) of zeolite were placed in 500-mL polyallomer centrifuge bottles with 100 mL of one of two surfactant solutions. One solution was made up to 0.45 mM for the initial concentration, which is one-half of the critical micelle concentration (cmc) of 0.9 mM (at 25 °C) (*22*), and therefore contained predominantly HDTMA monomers (sub-cmc). The other solution was two times the cmc or 1.8 mM for the initial concentration, where much of the HDTMA was in micellar form (super-cmc). Each surfactant solution was spiked with [^{14}C-methyl]HDTMA (American Radiolabelled Chemicals, Inc., St. Louis, MO) prior to the treatment step. The zeolite was treated with each HDTMA solution by batch methods to 50%, 100%, and 400% of ECEC, where 100% was assumed equal to 90 mequiv/kg zeolite. To do this, each sample was prepared by weighing the appropriate amount of zeolite into a 50-mL polyallomer centrifuge tube, and 40 mL of the appropriate solution was added. Each sample was prepared in duplicate, and appropriate solution and zeolite blanks were included in each batch. The solutions were shaken with the zeolite for 7 days at 25 °C, then the SMZ was centrifuged at 14500*g* for 30 min. Preliminary experiments showed that up to 7 days was required to obtain sorption equilibrium for the low-concentration solutions used. After the centrifuging step, 5 mL of supernatant was removed from each bottle for analysis of HDTMA and Br^-. ^{14}C-labeled HDTMA was determined using a Packard Tri-Carb liquid scintillation counter. The supernatants were analyzed for Br^- by high-performance liquid chromatography (HPLC). The surface tension was also measured to determine if the supernatants were above or below the cmc.

To measure chromate sorption, the samples were then spiked with 5 mL of either a 0.19 mM solution (for the more dilute monomer system) or a 1.9 mM solution (for the micelle system) of K_2CrO_4 (Baker Chemicals). The chromate-spiked SMZ was shaken for 24 h, a time previously found to be sufficient for equilibrium (*2*) and then centrifuged, and an aliquot of supernatant was removed as above. Samples were analyzed for Br^- and chromate by HPLC.

FT-Raman Sample Preparation. The unmodified zeolite was first saturated with sodium by shaking 40 g with 120 mL of 1 N, pH 5, sodium acetate buffer for 15 min. The samples were centrifuged at 14500*g* for 20 min, the supernatant was discarded, and the entire sequence was repeated two more times. This was followed by triple rinses with type I water and 95% ethanol and then air-drying.

The sodium-saturated zeolite was modified with HDTMA to a range of coverages from 0% to 310% of the ECEC. Surfactant modification consisted of shaking 5 g of zeolite with 20 mL of the selected HDTMA solution (between 0 and 70 mM) for 12 h at 25 °C. This amount of time was shown to be sufficient for complete reaction of HDTMA on zeolite for these solution concentrations (*23*). All initial solutions were above the cmc. The SMZ was centrifuged at 14500*g* for 30 min, and excess HDTMA solution decanted. The samples were then washed with 20 mL of type I water, centrifuged, and decanted as above.

The various samples of SMZ were then shaken for 24 h with 0.04 mM K_2CrO_4 in the ratio of 1 g of zeolite to 4 mL of solution. The samples were allowed to settle for 1 h, and excess solution was removed with a pipet. The SMZ−chromate was then rinsed for 30 s with 5 mL of the chromate solution, and the excess solution was removed with a pipet. This step was repeated two more times and was intended to reduce the concentration of HDTMA in the supernatant to prevent interference. A background check revealed that the 0.04 mM chromate solution was below the FT-Raman detection limit. Each SMZ−chromate sample was packed as a wet slurry into a nonfluorescing Nicolet NMR glass tube for FT-Raman analysis.

FT-Raman Spectroscopy. Solutions of 70 mM K_2CrO_4, 0.45 mM and 70 mM HDTMA, and wet slurries of SMZ and SMZ−chromate were analyzed using a Nicolet 910 FT-Raman spectrometer with a diode-pumped solid-state laser emitting at 1064 nm. Samples were loaded as a solution or wet slurry into 5 mm nonfluorescing Nicolet NMR tubes. The laser power was adjusted to 1.1 W. There were 3000 scans co-added for each spectrum at 1 cm^{-1} resolution. Wavenumber accuracy was ±1 cm^{-1}, and the range of operation was 4000−50 cm^{-1}. Background scans were taken of a 70 mM K_2CrO_4 solution to determine if solution chromate would interfere with the sorbed chromate spectrum, which it did not. Therefore, a 200 mM K_2CrO_4 solution at pH 7 and a 200 mM solution at pH 4 were used to produce the solution chromate spectra. The signal-to-noise criterion for peak existence was 3 standard deviations above the mean value of the noise. Band shifts of greater than 2 cm^{-1} were considered to be real changes in vibration energy values.

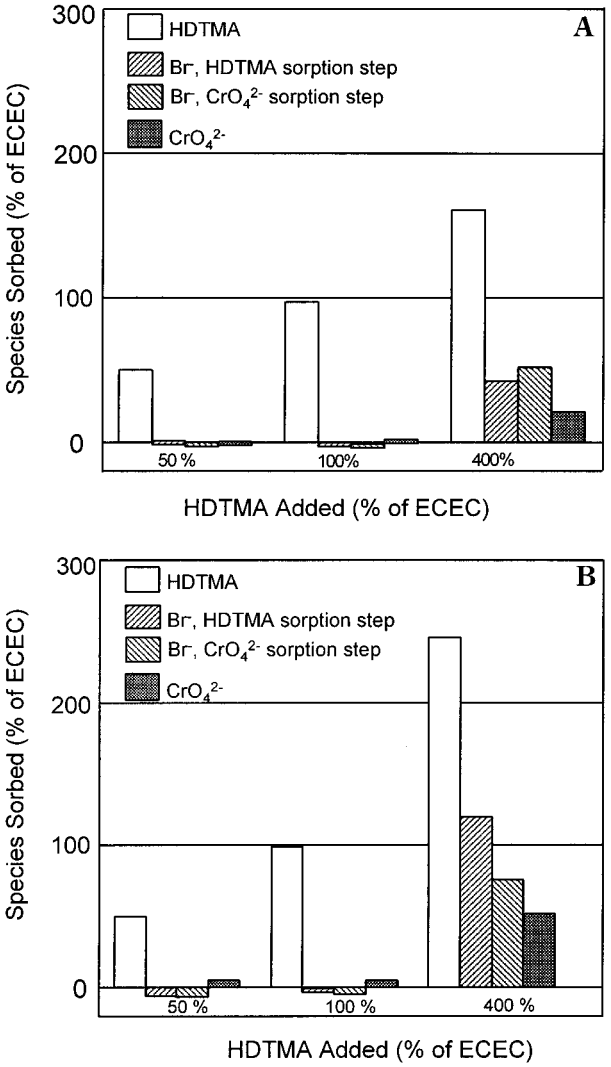

FIGURE 1. Equilibrium sorption data for (A) monomer (<cmc) and (B) micelle (>cmc) HDTMA sorption to clinoptilolite zeolite, with Br^- counterion data for the initial sorption step. Sorbed CrO_4^{2-} and Br^- concentrations are also shown for the subsequent CrO_4^{2-} spike step.

Results and Discussion

Sorption Data. The samples treated to 50 or 100% of the ECEC should exhibit an absence of a bilayer (i.e., a monolayer) of surfactant whether the surfactant is applied as monomers or micelles (*15*). The samples treated to 400% of ECEC were expected to produce a surfactant bilayer. Previous sorption studies showed that monomer solutions produce stable monolayers at less than the ECEC, but above the ECEC they produce less extensive bilayers than do micelle systems. Micelle systems readily form complete bilayers or extensive admicelles when treated above the ECEC (*15*).

Data for HDTMA sorption to zeolite and subsequent chromate sorption to the SMZ are shown in Figure 1, panels A and B. The plots also show millequivalent sorption of the original Br^- counterion, the remaining Br^- sorbed after CrO_4^{2-} treatment, and CrO_4^{2-} sorbed. Chromate was assumed to be sorbing as CrO_4^{2-}, based on previous experiments which showed pH values of about 7. Surface tension measurements (not shown) indicated that all of the solutions fell at or below the cmc after the HDTMA sorption step, a condition expected to correlate with complete HDTMA sorption (*15*). HDTMA sorption results were similar to those found in previous studies (*15*).

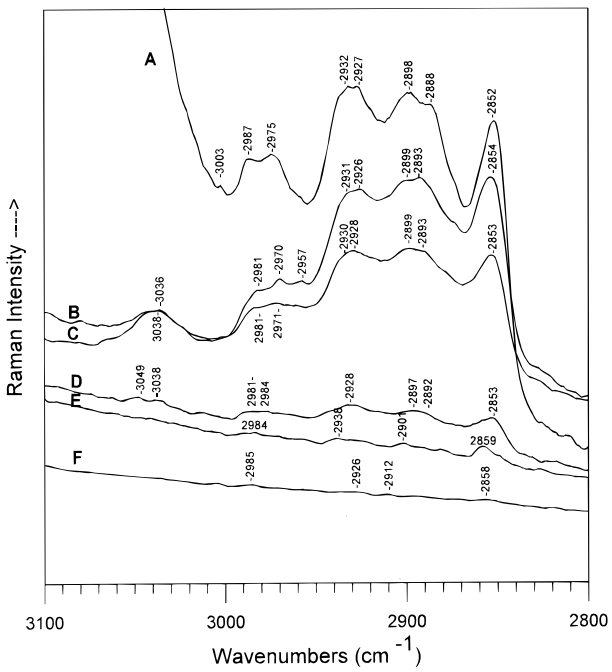

FIGURE 2. FT-Raman higher frequency spectra for (A) an HDTMA micelle solution, and HDTMA sorbed on clinoptilolite zeolite for a series of treatment levels: (B) 310% ECEC, (C) 230% ECEC, (D) 160% ECEC, (E) 80% ECEC, and (F) 60% ECEC.

HDTMA sorbed quantitatively in the 50% and 100% treatments while Br^- sorption was very low for these samples, indicating that no bilayer existed on the surface. Subsequent CrO_4^{2-} sorption was also extremely low, indicating that SMZ with a monolayer conformation does not readily sorb CrO_4^{2-}, as expected for a hydrophobic surface. Unmodified zeolite also does not sorb CrO_4^{2-} (*2*).

For the 400% treatment samples, HDTMA sorption was 160% and 246% of ECEC for the monomer and micelle systems, respectively. Initial bromide sorption was 120% of ECEC in the micelle system and 42% of ECEC in the monomer system. This indicates admicelle or bilayer formation in both systems; however, the monomer system bilayer is less complete and is probably in the form of patchy bilayers. Subsequent CrO_4^{2-} treatment resulted in chromate sorption equal to 20% and 52% of ECEC for the monomer and micelle systems, respectively. The mequiv of CrO_4^{2-} plus Br^- sorbed was 106% of the original mequiv of Br^- sorbed in the micelle system. A gain in Br^- sorption was noted, from 42% to 52% of ECEC in the CrO_4^{2-} sorption step of the monomer system, while total $Br^- + CrO_4^{2-}$ was 72% of ECEC. The total sorbed anion equivalents were close to the equivalents of surfactant adsorbed above the ECEC, with a slight positive gain of anions on the surface during the chromate sorption step. These results indicate that anion exchange is a reasonable mechanism for CrO_4^{2-} sorption and that CrO_4^{2-} sorption is most favored in those samples where a full bilayer exists.

FT-Raman Spectra Assignment of Sorbed HDTMA Band Shifts. The higher frequency bands corresponding to the CH_3-N^+, CH_3-R, and CH_2 stretching regions are shown in Figure 2 and listed in Table 1 for a range of coverages of sorbed HDTMA. Also shown is the spectrum for a 70 mM HDTMA micelle solution. The results correlate well with reported literature values (*11, 14*). Band intensity is reduced with reduced surface coverage, and so the lowest treatment levels are not shown (*5*). Some peaks related to CH_3-N^+ stretching (head group interactions), CH_3-R stretching, and CH_2 stretches (chain interactions) were not detected at lower treatment levels because of insufficient signal-to-noise ratios. Interestingly, parallel vibrations did not always disappear

TABLE 1. FT-Raman High-Frequency Data for Sorbed HDTMA at Various Treatment Levels for the Spectra Shown in Figure 2

tentative assignment	Raman bands, cm^{-1} HDTMA treatment level (percentage of ECEC)[a] 60%	80%	160%	230%	310%	HDTMA 70 mM (micelles)	reference[a,b] 100 mM (micelles)
CH_2 s-stretch[a,b]	2858 w	2859	2853	2853	2854	2852	2854
CH_3−R s-stretch ?			2892 sh	2893 sh	2893 sh	2888 sh	
CH_2 a-stretch[b,c]	2912	2901 w	2897	2899	2899	2898 b	2890[c]
CH_2 a-stretch[d]?	2926 w	2926 w	2928 sh	2928	2926	2927	2930[d]
CH_2 a-stretch[a,c]		2938	2930	2930 sh	2931 sh 2957	2932	2935
CH_3-N^+ s-stretch[a,b]			2971 sh	2971	2970	2975	2974
CH_3-N^+ a-stretch[a]	2985	2984	2981−2984 b	2981 sh	2981	2987 3003	2987
CH_3-N^+ a-stretch[b]			3038 3049	3038 b	3036	3047	3042

[a] Ref *11*. [b] Ref *14*. [c] Suga et al. (*11*) characterize this as a CH_3−R s-stretch. [d] Suga et al. (*11*) characterize this as a surface-enhanced Raman band. [e] w, weak; sh, shoulder, b, broad peak.

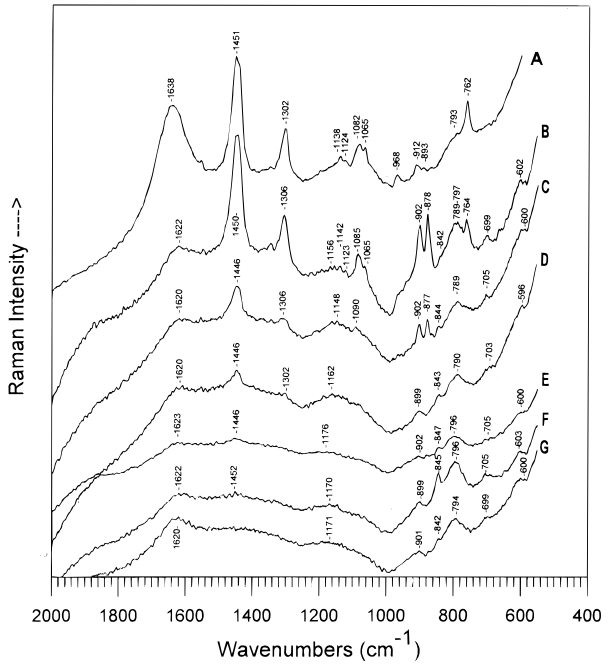

FIGURE 3. FT-Raman lower frequency spectra of (A) HDTMA micelles, and HDTMA sorbed on clinoptilolite zeolite for a series of treatment levels: (B) 310% ECEC, (C) 160% ECEC, (D) 80% ECEC, (E) 60% ECEC, (F) 20% ECEC, and (G) unmodified clinoptilolite zeolite. Spectra shown are from the HDTMA−chromate treatment system.

with reduced loading. For example, the CH_3-N^+ a-stretch is retained, but shifts to 2985 cm^{-1} for the 60% treatment level, while the CH_3-N^+ s-stretch was not detected. The CH_2 a-stretch at 2926 cm^{-1} was retained, but the CH_2 a-stretch at about 2930 cm^{-1} was not.

Lower frequency spectra for various HDTMA treatment levels are shown in Figure 3, and the band assignments are listed in Table 2. Also listed are the lower frequency band assignments for a reference 100 mM HDTMA micellar solution (*11, 14*). Loss of band resolution occurred with reduced coverage, but to a lesser extent than for the higher frequency portion of the spectrum. Band assignments for the alkyl (tail group) chain, the methyl head group, and other features in both the high- and low-frequency ranges are discussed below by group.

Alkyl Chain Assignments—Solution Micelles and Admicelles. There is a strong correlation between many peaks for the micellar HDTMA solution and the 160%, 230%, and 310% treatment-level samples (Figures 2 and 3), which indicates structural similarities between micelles in solution and admicelles. On the basis of peak shift comparisons pertinent to the alkyl chain, it is interpreted that the tail groups in admicelles are only slightly less structured and interfingered than those in solution micelles. Peak shifts (δ) from the HDTMA solution values were no more than 2 cm^{-1}, the criterion for distinguishing a shift between peaks. High-frequency bands that illustrate this similarity are the CH_2 s-stretch (2852 cm^{-1}, $\delta = +1, +2$), the CH_2 a-stretch (2898 cm^{-1}, $\delta = \pm 1$), and the CH_2 a-stretch (2932 cm^{-1}, $\delta = -1, -2$), which are essentially the same for both sorbed bilayers/admicelles (160−310%) and the solution system (Figure 2, Table 1). The largest difference occurs in the CH_3−R s-stretch [others (*15*) identify this as a CH_2 stretch], which shifts from 2888 cm^{-1} for the micelle solution to 2893 cm^{-1} for the 310% treatment level ($\delta = +5$). This indicates more gauche conformers, where micelles on the surface have less ordered or structured tail groups than in solution. Because this shift only occurs for one of the bands, this is potentially a minor effect that may occur only for the terminal part of the tail group. The peak disappears with reduced loading, so no correlation with adsorbed monomers can be made.

In the lower frequency range (Figure 3, Table 2), four tail group bands listed for the 310% treatment level (admicelles) corresponded very closely to those found for solution micelles, including one band at 1138 cm^{-1} in solution, which was listed but not assigned in the literature (*14*). These bands include the C−C stretch (1065 cm^{-1}, $\delta = 0$), the CH_2 twist (1302 cm^{-1}, $\delta = +4$), and the CH_2 scissor (1451 cm^{-1}, $\delta = -1$) for tail group assignments as well as a tentative assignment of the head group $C-N^+$ stretch (head group−tail group bond, 762−764 cm^{-1}, $\delta = +1$). Few significant shifts were noted for HDTMA bands between treatment levels in this range of the spectrum, with the exception of the C−C bands for 160% and 230% treatments ($\delta = +8, +10$). All of the bands disappeared at some reduced loading level, e.g., below 60% ECEC coverage.

Alkyl Chain Assignments—Sorbed Admicelles and Monomers. In Figure 2, we see a shift to higher frequency with lower coverage for the CH_2 s-stretch, for example, in the change from 2853 to 2858 cm^{-1} ($\delta = +5$) between the 160% and 80% treatment levels (Table 1). A similar change is noted for the CH_2 a-stretch between the 160% level (2898 cm^{-1}) and the 60% level ($\delta = +15$). These changes may be associated with increased twisting or bending of the chain when the admicelle structure is disassembled at lower treatment levels. In Figure 3, the C−C stretch (1085 cm^{-1}) in the 310% treatment level shifted to 1090 cm^{-1} and weakened in the 160% treatment level before disappearing entirely at lower treatment levels (Table 1). This shift as an

TABLE 2. FT-Raman Low-Frequency Data for Sorbed HDTMA, Unmodified Clinoptilolite Zeolite, and Sorbed Chromate at Various Treatment Levels for the Spectra in Figures 3 and 5

tentative assignment	Raman bands, cm^{-1}								
	HDTMA treatment level (percentage of ECEC)[a]							HDTMA 70 mM (micelles)	reference[b] 100 mM micelles
	0%	20%	60%	80%	160%	230%	310%		
zeolite	600	603	600	596	600	597	602		
zeolite	699	705	705	703	705	698	699		
$C-N^+$ stretch[a,b]						763	764	762	760
zeolite	794	796	796	790	789	786	789−797		
						794			
						815 sh		793 sh	
zeolite	842 sh	845	847	843 sh	844 sh		842 sh		
chromate					877	878	878		
								893	891
chromate or zeolite	901	899	902	899	902[c]	904[c]	902[c]		
CH_3 rock,								912	912
CN^+ stretch[b]								968	970
C−C stretch[b,d]					1090	1092	1065 sh	1065	1064
							1085	1082	1084
							1123	1124	1122
							1142	1138	
zeolite and /or water	1171 b	1170 b	1176 b	1162 b	1148 b	1144	1156 b		
						1164			
						1199			
CH_2 twist				1302	1306	1306	1306	1302	1302
CH_2 scissor[a,b]		1452	1446	1446	1446	1451	1450	1451	1450
zeolite and/or water	1620 b	1622 b	1623 b	1620 b	1620 b	1621	1622 b	1638	

[a] Ref *11*, for sorbed HDTMA (surface-enhanced Raman spectrum). [b] Ref *14*. [c] Due to chromate overwhelming zeolite peak. [d] Sun et al. (*25*) assign a peak at 1065 cm^{-1} as a C−C symmetric stretch and a peak at 1121 cm^{-1} as a C−C antisymmetric stretch. [e] w, weak; sh, shoulder; b, broad peak.

indication of the C−C bonds paralleling the surface, in conjunction with weakening of the CH_2 twist and scissor bands (*14*). The CH_2 twist (1302−1306 cm^{-1}), however, shifts higher ($\delta = +4$) and then disappears below the 80% treatment level, while the CH_2 scissor (1446 cm^{-1} at 160% level) shifts higher and persists weakly at the 20% level ($\delta = +6$).

These observations indicate disorder in monolayer chains, quite different from the organized trans-conforming monolayer described by Sun et al. (*25*) for HDTMA sorbed on a silver electrode. Disorder also has been associated with dry systems (*8*). Our interpretation corresponds well with previous atomic force microscope observations of disorganized HDTMA monomers on the zeolite surface (*4*). Disorganization may be enhanced by the molecularly rough zeolite surface, as opposed to the relatively smooth metal surfaces used by others (*11, 14*). Surfactant orientation also may depend on the quantity of surfactant on the surface (*4, 26−28*), with close horizontal contact (less ordering) between the surfactant and surface at low loading levels and with a perpendicular orientation (greater ordering) at higher loading levels.

Figure 4 shows a schematic of the resulting structural changes during HDTMA sorption based upon the FT-Raman data. Sorbed micelles exhibit slightly more tail group disorder and less interfingering of tail groups than do solution micelles, based on peak shift data. This is interpreted to result from interaction with the rough zeolite surface. Sorbed monolayers at higher loading levels are more structured than monomers sorbed at low coverages. Monomers at any loading level exhibit more disorder than admicelles. These monomers may interact with the zeolite surface or perhaps "coil up" when other tail groups are not available for hydrophobic interactions.

Head Group Assignments. The bands associated with the symmetrical and asymmetrical CH_3-N^+ stretches (Figure 2, Table 1) show distinct differences between solution and adsorbed HDTMA (310% treatment level). The loss of the symmetrical stretch (2970 cm^{-1}), with retention of the asymmetrical stretch in the CH_3-N^+ group (2970−2985 cm^{-1}) below the 160% treatment level may indicate an alteration of the head group bond on the surface between lower and higher loading levels.

The sorbed head group CH_3-N^+ a-stretch and s-stretches all shift to a lower frequency at the 310% loading level when compared with solution head group bands. This indicates less hydration for sorbed head groups than for those in solution. This same lower frequency shift occurs between solution HDTMA and wet films (*11, 14*). Interestingly, a reversal in the trend then occurs from the 80% to 60% treatment levels, where the peaks shift higher again. The corresponding peak in the 160% level is broad, so this relative shift is indistinct but may indicate more water available to the headgroups as monolayer density is decreased. Nitrogen bands in pyridine−water mixtures also shift to higher frequencies upon hydration (*5, 18*). Water has been noted to exist between head groups and silver island surfaces in previous studies of sorbed HDTMA monolayers (*11*).

FT-Raman Band Assignments for Chromate. Figure 5 shows a comparison among the chromate bands for a K_2CrO_4 solution (200 mM, pH 7), a K_2CrO_4 solution (200 mM, pH 4), an HDTMA−chromate solution [70 mM $(HDTMA)_2CrO_4$], and the CrO_4^{2-}−SMZ (310% treatment level, pH 7.5) spectrum. The spectrum for an unmodified zeolite equilibrated with 200 mM K_2CrO_4 solution is also shown. Chromate in solution at pH 7 (Figure 5 C) produces a strong band at 847 cm^{-1} and a shoulder at 887 cm^{-1} corresponding to the ν_1 (Cr−O, symmetric stretch) and ν_3 (Cr−O, asymmetric stretch) transitions, respectively (*29*). These are two of four normal modes for free chromate tetrahedral anions (*29*). These bands are unchanged when chromate is mixed with HDTMA micelles in solution (Figure 5D). At a pH > 6, CrO_4^{2-} is the dominant aqueous species (Figure 5C), while at pH < 6, dichromate ($Cr_2O_7^{2-}$) becomes increasingly important. When the pH is decreased below 6 for a chromate solution (Figure 5B), an intense terminal stretching frequency for dichromate ($Cr_2O_7^{2-}$) is seen in the spectrum at 902 cm^{-1} (*30, 31*). This frequency also has been noted in spectra for solid Na_2CrO_4. This frequency occurs in the solid as the symmetry is reduced

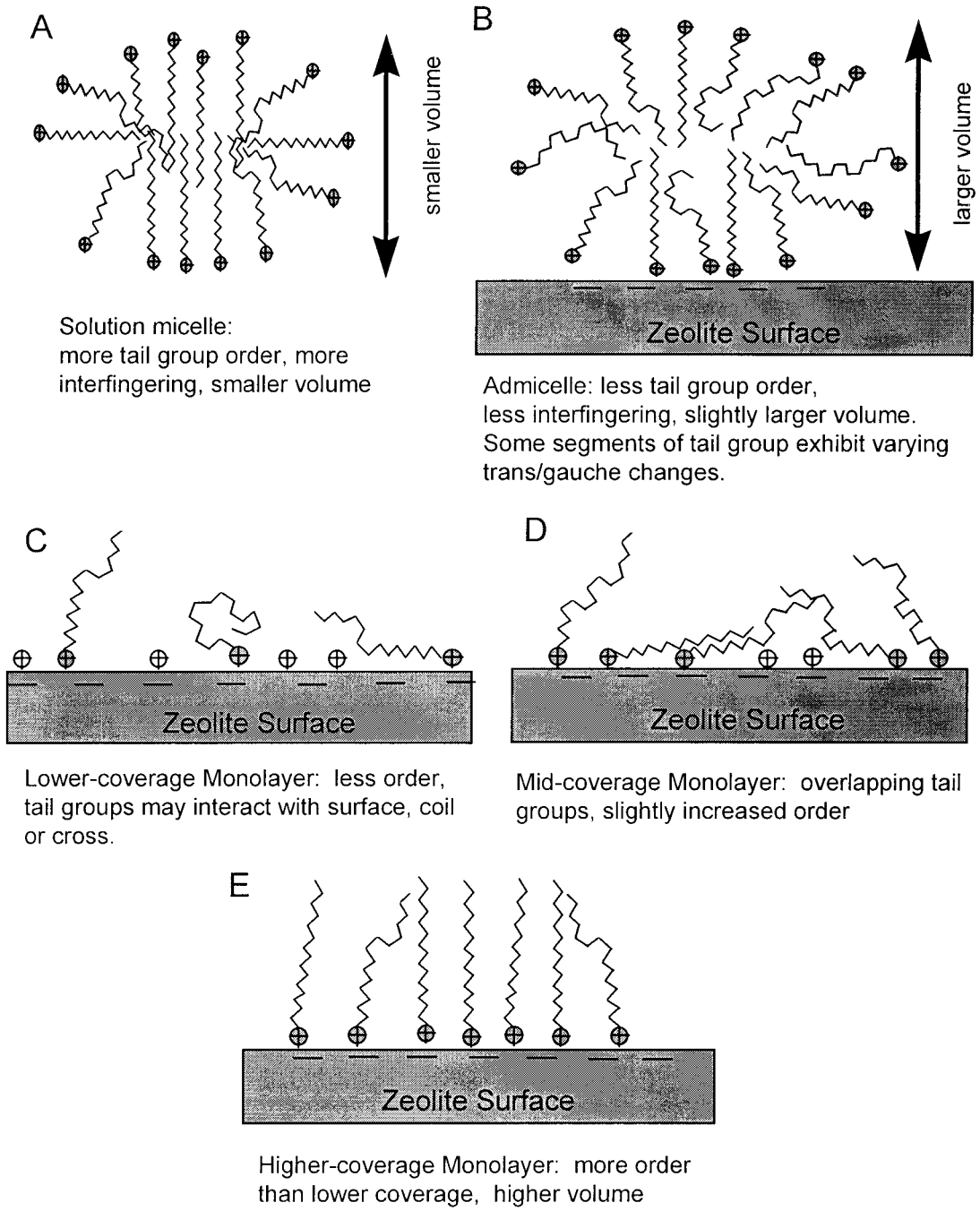

FIGURE 4. Two-dimensional schematic of HDTMA sorbed as micelles or monomers on the zeolite surface, describing the effects of sorption on tail group disorder. Although not illustrated, the third dimension of the surfactant structure, surface roughness, and time also affect the amount of disorder in the surfactant tail groups.

from that of the solution tetrahedra and may indicate symmetry reduction for dichromate as well (*29*).

The chromate bands are clearly altered when chromate is sorbed to SMZ. Reduction of Cr(VI) to Cr(III) does not occur with sorption on SMZ, as shown in previous studies (*2*). Sorbed chromate is visible in the spectrum as two strong bands at 902 and 878 cm^{-1} (Figure 5 A; Table 2). These bands only were seen for chromate sorbed to SMZ treated with HDTMA at the 310−160% treatment levels and are unrelated to zeolite, HDTMA, or water bands, although there is a weak, broad band in the clinoptilolite spectrum at about 901 cm^{-1} that is obscured by the chromate peak (Figure 3G). The band at 902 cm^{-1} corresponds to the presence of $Cr_2O_7^{2-}$ on the zeolite surface (*30, 31*) and again is likely the result of a reduction of tetrahedral symmetry in the near-surface environment. Oligomerization of surface-sorbed chromate to dichromate was unexpected at the slightly basic conditions of these experiments. Huang and Butler (*32*) list bands at 854 (ν_1), 880 (ν_3), and 907 cm^{-1} (ν_3) for solid K_2CrO_4, while Bostic et al. (*33*) list a ground-state vibration at 853 cm^{-1} for aqueous K_2CrO_4. Although adsorbed chromate exhibits the two ν_3 vibrations much like solid chromate, the broadened line widths are more consistent with solution phase species. A full symmetry analysis, however, is beyond the scope of this study.

The lack of chromate bands when aqueous chromate solution is equilibrated with unmodified zeolite (Figure 5F) confirms that there is no sorption in the absence of bound HDTMA (*2*). In addition, as shown above, chromate does not sorb well to SMZ modified to levels less than 100% of the

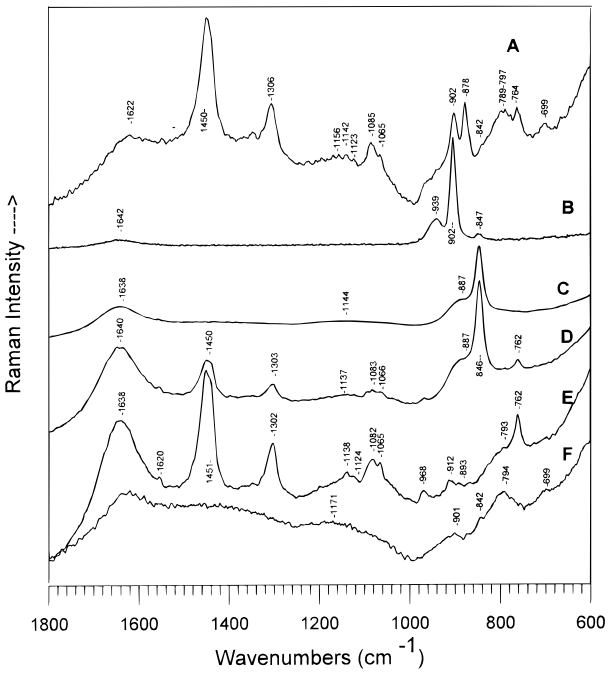

FIGURE 5. FT-Raman lower frequency spectra for (A) CrO_4^{2-} sorbed on 310% ECEC−SMZ, (B) aqueous K_2CrO_4 (200 mM, pH 4), (C) aqueous K_2CrO_4 (200 mM, pH 7), (D) aqueous $(HDTMA)_2CrO_4$ (70 mM), (E) aqueous HDTMA−Br^- micelles (70 mM), and (F) unmodified clinoptilolite zeolite that was equilibrated with 200 mM CrO_4^{2-}.

ECEC (Figures 1 and 3). It is interesting to note that, regardless of whether chromate or Br^- is the HDTMA counterion in aqueous solution, there is no effect on bands related to HDTMA head group or tail group conformation (Figure 5D,E).

To test whether the dimerization of chromate was caused by high concentrations on the surface of the zeolite, chromate was sorbed to a quaternary ammonium cationic exchange resin (BioRad AG-1-X8) under conditions similar to chromate sorption on SMZ. The resin should behave similarly to the quaternary ammonium head group of HDTMA. No formation of $Cr_2O_7^{2-}$ was noted in the Raman spectrum of this model exchange phase (data not shown). Hence, we conclude that the appearance of dichromate on SMZ was not due to a shift in the CrO_4^{2-}−$Cr_2O_7^{2-}$ equilibrium induced by high local concentrations of chromate. Either the chromate sorption density is much greater on the SMZ than on the resin or specific chromate−SMZ interactions result in formation of $Cr_2O_7^{2-}$.

The other chromate-related peak at 878 cm^{-1} (Figure 5A) is more difficult to assign but is most likely ascribable to a shift in the ν_1 Cr−O symmetric stretch resulting from a surface-bound chromate species. First, it is unlikely that all the chromate is oligomerized to dichromate (based upon the sorption data which shows a near, but not exact, balance in the chromate−bromide exchange). An equilibrium likely exists between the two species near the surface. Second, large shifts of 50 cm^{-1} for CrO_4^{2-} sorbed to metal surfaces have been described previously (*30, 31*). In the presence of excess surfactant, the relative acidity of Lewis acid sites on the zeolite surface may be enhanced through reduction of the amount of water present at the surface. When CrO_4^{2-} penetrates the bilayer, it can act as an electron donor to these sites. The strong shift in the peak is typical of other Lewis bases such as pyridine (*18, 19*). Both electron donation and anion exchange require the presence of sufficient sorbed surfactant, making it difficult to distinguish between the two possibilities. It appears that ion exchange is the dominant sorption mechanism, but surface-enhanced oligomerization and Lewis acid interactions also contribute to the sorption process.

In summary, we have shown that Raman spectroscopy can be a powerful probe to investigate complex interactions at the surface−water interface. It is evident that changes in surfactant ordering on the zeolite surface versus solution micelles give rise to synergistic sorption processes for Cr(VI) involving both surface-bound CrO_4^{2-} and $Cr_2O_7^{2-}$ species.

Acknowledgments

We thank the three anonymous reviewers for their comments. This study was supported by The Clay Minerals Society, the Oak Ridge Institute for Science and Education, U.S. DOE Contract DE-AR21-95-MC32108 through the Morgantown Energy Technology Center, Financial Assistance Award DE-FC09-96SR18546 from DOE to the University of Georgia Research Foundation, and ERDA/WSRC Subcontract AA46420T. The support of the Advanced Analytical Center for Environmental Sciences at the Savannah River Ecology Laboratory, including Brian Teppen, John Seaman, and Paul Bertsch, is acknowledged. Emily Keene and Z. Li of New Mexico Tech performed the sorption and laboratory studies.

Literature Cited

(1) Bowman, R. S.; Haggerty, G. M.; Huddleston, R. G.; Neel, D.; Flynn, M. M. In *Surfactant-Enhanced Subsurface Remediation*; Sabatini, D. A., Knox, R. C., Harwell, J. H., Eds.; ACS Symposium Series 594; American Chemical Society: Washington, DC, 1995; pp 54−64.
(2) Haggerty, G. M.; Bowman, R. S. *Environ. Sci. Technol.* **1994**, *28* (3), 452−458.
(3) Neel, D.; Bowman, R. S. *Proceedings of the New Mexico 36th Annual Water Conference*, November 7−8 1991, Las Cruces, New Mexico; 1992; pp 57−61.
(4) Sullivan, E. J.; Hunter, D. B.; Bowman, R. S. *Clays Clay Miner.* **1997**, *45* (1), 42−53.
(5) Burch R.; Passingham, C.; Warnes, G. M.; Rawlence, D. J. *Spectrochim. Acta* **1990**, *46A* (2), 243−251.
(6) Umemura, J.; Cameron, D. G.; Mantsch, H. H. *J. Phys. Chem.* **1980**, *84*, 2272−2277.
(7) Kellar, J. J.; Young, C. A.; Knutson, K.; Miller, J. D. *J. Colloid Interface Sci.* **1990**, *144* (2), 381−389.
(8) Kung, K. S.; Hayes, K. F. *Langmuir* **1993**, *9*, 263−267.
(9) Grasselli, J. G.; Snavely, M. K.; Bulkin, B. J. *Chemical Applications of Raman Spectroscopy*; John Wiley & Sons: New York, 1981; 198 pp.
(10) Hendra, P. J.; Jones, C.; Warnes, G. M. *Fourier Transform Raman Spectroscopy, Instrumentation and Chemical Applications*; Ellis Horwood: New York, 1991; 259 pp.
(11) Suga, K.; Bradley, M.; Rusling, J. M. *Langmuir* **1993**, *9*, 3063−3066.
(12) Vincent, J. S.; Levin, I. W. *Biophys. J.* **1991**, *59*, 1007−1021.
(13) Levin, I. W.; Lewis, E. N. *Anal. Chem.* **1990**, *62* (21), 1101−1111.
(14) Dendramis, A. L.; Schwinn, E. W.; Sperline, R. P. *Surf. Sci.* **1983**, *134*, 675−688.
(15) Sullivan, E. J.; Carey, J. W.; Bowman, R. S. Thermodynamics of cationic surfactant sorption onto clinoptilolite, *J. Colloid Interface Sci.* In review.
(16) Hendra, P. J.; Passingham, C.; Warnes, G. M.; Burch, R.; Rawlence, D. J. *Chem. Phys. Lett.* **1989**, *164*, 178−184.
(17) Farmer, V. C. *Soil Sci.* **1971**, *112* (1), 62−68.
(18) Jakupca, M. R.; Dutta, P. K. *Anal. Chem.* **1992**, *64*, 953−957.
(19) Chipera, S. J.; Bish, D. L. *Powder Diffr.* **1995**, *10*, 47−55.
(20) Carey, J. W. Los Alamos National Laboratory, personal communication, 1995.
(21) Ming, D. W.; Dixon, J. B. *Clays Clay Miner.* **1987**, *35* (6), 463−468.
(22) Israelachvili, J. N. *Intermolecular and Surface Forces*, 2nd ed.; Academic Press: San Diego, CA, 1991; 450 pp.
(23) Sullivan, E. J.; Bowman, R. S.; Haggerty, G. M. In *Spectrum 94, Proceedings of Nuclear and Hazardous Waste Management International Topical Meeting*, August 14−18, 1994, Atlanta, GA; Vol. 2, pp 940−945.
(24) Diem, M. *Introduction to Modern Vibrational Spectroscopy*; John Wiley & Sons: New York, 1993; 285 pp.
(25) Sun, S.; Birke, R. L.; Lombardi, J. R. *J. Phys. Chem.* **1990**, *94*, 2005−2010.

(26) Ter-Minassian-Saraga, L. *Adv. Chem. Ser.* **1964**, *43*, 232.
(27) Bijsterbosch, B. H. *J. Colloid Interface Sci.* **1974**, *47* (1), 186−198.
(28) Chen, Y. L.; Chen, S.; Frank, C.; Israelachvili, J. *J. Colloid Interface Sci.* **1992**, *153* (1), 244−265.
(29) Pope, S. J. A.; Butler, Y. D. *Spectrochim. Acta A* **1995**, *51*, 2027−2037.
(30) Feilchenfeld, H.; Siiman, O. *J. Phys. Chem.* **1986**, *90*, 2163−2168.
(31) Feilchenfeld, H.; Siiman, O. *J. Phys. Chem.* **1986**, *90*, 4590−4599.
(32) Huang, Y.; Butler, I. S. *Appl. Spectrosc.* **1990**, *44* (8), 1326−1328.
(33) Bostic, J. M.; Carriera, L. A.; Antcliff, R. R. *J. Raman Spectrosc.* **1990**, *21*, 601−605.

Received for review October 13, 1997. Revised manuscript received March 18, 1998. Accepted April 9, 1998.

ES9708981